

Automated Threat Detection for Disaster Response Teams Using UAV Platforms

Andrew Schweig
Tufts University
Andrew.Schweig@tufts.edu

Abstract – In this paper, we present a sensor system, mountable on a commercially available quadcopter unmanned aerial vehicle (UAV). The system comprises of real-time video, radiation detection, and vehicle telemetry. We present methods of integrating sensor hardware and software with existing frameworks. The system is intended for use by disaster first response teams to prevent injury or loss of human life during site surveillance.

I. Introduction

At a disaster site, the first responders must identify potential hazards before moving in to rescue survivors or attempt hazard containment/clean-up. Without advance knowledge of the site, responders are presented with many unseen threats, including chemical and radiological sources. A UAV can navigate these dangerous sites and relay information to the responders before any humans enter the site. Previous systems incorporate static images or real-time video only. Previous research in 2013 by Davis, Pittaluga, and Panetta [1] provided the starting point for this project by using video detection algorithms for facial recognition. Additional information of radiation sources adds an additional layer of safety.

II. Background Information

A. Geiger-Müller Tube

Geiger-Müller tubes are devices used within a Geiger-Müller instrument (Geiger counter) to detect alpha- or beta-particles and gamma-rays. The tube is constructed of metal filled with inert gas. The tube has wire leads or end terminals that function as cathode and anode; however, some tubes can be operated in either orientation. The Canberra Industries T2417AC¹ tube used in our sensor is unidirectional, with the anode at the core of the

device and the cathode lead connected to the tube exterior. The T2417AC tube (fig. 1) was chosen for its high sensitivity and low weight and size. The tube has a 4 cm long, 1 cm diameter cylindrical detection window and weighs 8.0 g. Attached are two aluminum bars known as “energy wraps.” These bars filter out lower energy particles to maintain a consistent count output for any energy of radiative particles/rays. This is desirable, since counts per minute (cpm) is an effective measure of total amount of radiation occurring, rather than dose amount. Dosimeters or radiation badges are necessary to measure dosage.²

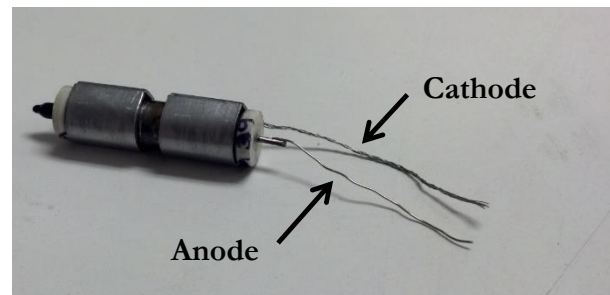


Fig. 1: T2417AC Geiger-Müller tube with energy wraps

Under normal operating conditions at room temperature and biased at 575 V (applied at the anode of the device), this tube has a sensitivity of 450 cpm in a radiative field of 1 milliRoentgen per hour (mR/hr) produced by Cesium-137 (¹³⁷Cs). The sensitivity of a Geiger tube is a linear measurement that relates radiation over time to cpm. That is, in a 1 mR/hr radiated field, the tube produces 450 cpm, and in a 2 mR/hr field, 900 cpm are measured, and so on. This allows for measurable detection at very low radiation levels and is also rated to have distinguishable results at up to and exceeding 6.9

¹ See Appendix for detailed specifications. Additional information at <http://www.canberra.com/products/detectors/detectors-geiger-mueller.asp> (listed as T2417A)

² See <http://www.remm.nlm.gov/civilian.htm> for information on dosimeters

million cpm (115200 counts per second (cps), the maximum our current digital system supports). This corresponds to a radiation rate of 15.36 R/hr or 135.2 Gy/hr if directly absorbed.³ An instantaneous absorption of 5 Gy in air is lethal to the average human [2][3]⁴. The knowledge that anywhere near this dosage of radiation could potentially be absorbed in a single area is more than enough to mark an area as hazardous to human health and require use of personal dosimeters to accurately monitor responders' safety [4].⁵

To power our sensor's Geiger-Müller tube with the requisite 575 V, we created a tunable high-voltage kickback generator⁶ (fig. 2) powered by the drone's on-board battery via a 5 V output.

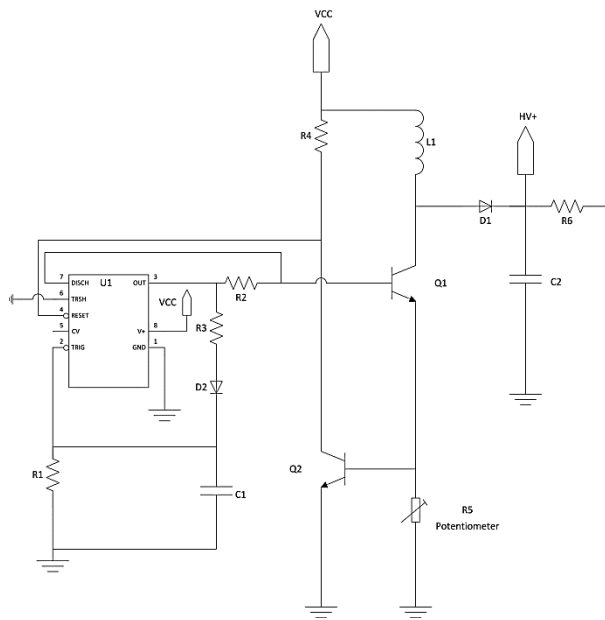


Fig. 2: High-voltage generator circuit⁷

At the core of the circuit is a 555 timer integrated circuit (IC). The timer functions as a pulse generator: when the trigger (TRIG) pin is brought to a low voltage, the output (OUT) generates a logical high (+5 V) square pulse; when the discharge (DIS) pin is brought high, the output returns to low voltage; if the reset (RESET) is

triggered by a low voltage, the IC shuts down, producing a low voltage at OUT.

Our design functions by allowing OUT to begin at low voltage, keeping TRIG low. This causes OUT to rise to 5 V. As this happens, current flow through R3 and D2, charges capacitor C1. Once charged, the current flows through R1, creating a high voltage at TRIG to prevent retriggering of the pulse. The pulse at OUT supplies enough voltage through R2 to the base of Q1 to reach the binary junction transistor (BJT) threshold voltage and switch it on. With Q1 on, current gradually begins to flow through L1. When enough current flows through L1, a voltage appears across R5, switching on Q2. The current flow through R4 and across Q2 causes a low voltage at RESET, turning off the IC. With the voltage at OUT now low, Q1 switches off. With a means of current flow to ground for the current through L1 removed, the current through the inductor should drop to zero. However, since inductors impede changes in current, the electromagnetic field stored in L1 manages to force its way across the semiconductor capacitance between the collector and emitter of Q1. When all current (and therefore charge) from L1 is stored in this capacitance, there is enough voltage⁸ across Q1 to allow D1 to operate in forward biased mode. Current flows from Q1, through the diode, and into C2. Since the pulses from the IC are only microseconds long (switching time for Q1 and thus current through L1), immense current is stored in Q1.⁹ The capacitance of C2 is orders of magnitude less than the capacitance of Q1, so the voltage at HV+ becomes several hundred volts. This voltage is used to power the Geiger-Müller tube across R6. Once the timer IC has been reset, C1 discharges through R1 until TRIG is again brought low, restarting the cycle.

B. Geiger Counter

To operate a Geiger-Müller tube, a high voltage is effected across the tube, with the higher potential at the anode. When not in the presence of radiation, a Geiger tube has high resistance (between 1 MΩ and 10 GΩ) and impedes current flow¹⁰. When no radiation is detected, the cathode of the Geiger tube is held at ground, so Q3 remains off (fig. 3). When a

³ 115.07 mR/hr fully absorbed in air is equal to 1 mGy/hr

⁴ Background information obtained from <http://www.epa.gov/radiation/>

⁵ See http://www.firstresponder.gov/Saver/RadiationDosimeters_TN.pdf for information on first responder dosimeters

⁶ Modified design inspired by that of Jeff Keyser (CC BY-SA): http://mightyohm.com/files/geiger/geiger_sch_fixedR5R6.png

⁷ See Appendix for bill of materials and larger image

⁸ Voltage of a capacitor is $V_c = \frac{q}{c}$

⁹ Current through an inductor is $i = \frac{1}{L} \int V_L dt$, where V_L is the voltage and L is inductance

¹⁰ See http://webfiles.ehs.ufl.edu/rssc_stdby_chp_4.pdf for more information on Geiger-Müller tube theory

radiative particle or ray strikes the surface of the tube, a small amount of gas molecules becomes ionized, creating a positive ion and a negative free electron. The electrons flow towards the anode in the center of the tube, ionizing more molecules as they collide at high energy. The resulting electron avalanche ionizes all gas around the anode within a few microseconds, causing current to flow out of the tube. After this pulse of current, the positive ions now near the cathode counteract the high electric field caused by the potential difference between electrodes, allowing the electrons to be reclaimed by the positive ions. A Geiger counter measures the current flow from the electron avalanche and presents the information in “counts.” To transition from current flow during a radiative event detection, a Geiger counter must display or convey the current as a count. A simple method is to measure a voltage across an external resistor. Our method uses a single BJT to drop the device’s output voltage to ground whenever a radiative event is detected. The flow of electrons causes a voltage to appear across R7 and R8, turning Q3 on. The current flowing through the transistor pulls the output low from 5 V. The output represents a constant binary 1 (5 V) until radiation is detected, showing a momentary binary 0 (0 V). At these values, the output is in binary format, readable with a high logic level of 5 V.

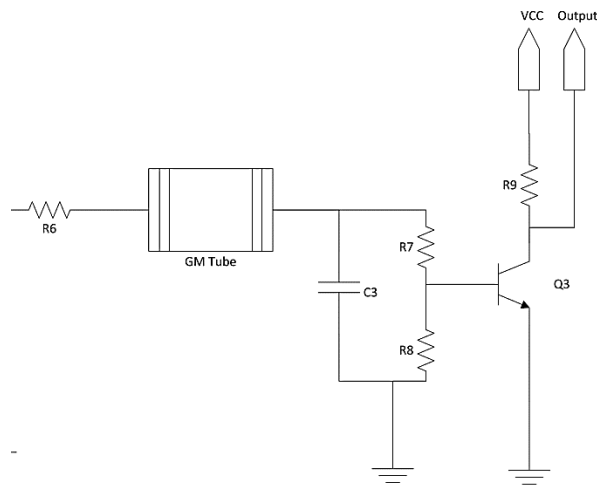


Fig. 3: Output stage of radiation detection circuit

All versions of our sensor were tested against a small sample of Americium-241 (^{241}Am) found in a commercial home smoke detector. ^{241}Am is an extremely lowly radioactive isotope that produces

little to no risk of harm for humans.¹¹ The isotope decays by low-energy alpha emission (stopped by clothing or several cm in air) and low amounts beta emission, which we measured with our sensor.

C. UAV Quadcopter

To carry the payload of sensors, a commercially available drone system was selected. The DraganFlyer Guardian¹² from DraganFly Innovations Inc. (fig. 4) was selected for its battery life, payload limit, size, and software customization.



Fig. 4: DraganFlyer Guardian

The UAV has a quadcopter configuration: four boom arms extend from the body and hold a single brushless DC motor with attached rotor blade. Legs below the motors keep the body and underhanging payload off the ground. The drone measures 71 cm in diameter with a height of 25 cm. A maximum payload size of 420 g allows for several sensors to be added to the payload area. This particular model includes a GoPro Hero 3 video camera with dual-axis gyro-stabilized mount (fig. 5) for receiving a live video feed. The stabilization is realized using two brushless DC motors and drone processor-based feedback control to correct for changes in drone roll and pitch. The camera and mount weigh 300 g when secured to the drone, leaving 120 g for our sensor package. A maximum flight time of 30 minutes gives a practical time window for site surveillance. A fail-safe activates at low battery to automatically safely land the drone.

¹¹ See <http://www.bt.cdc.gov/radiation/isotopes/americiam.asp> for safety information

¹² See Appendix for detailed specifications. Additional information at <http://www.draganfly.com/uav-helicopter/draganflyer-guardian/index.php>

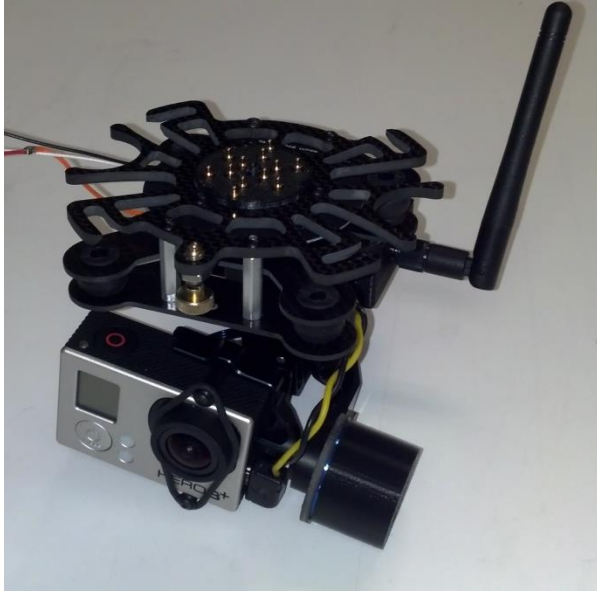


Fig. 5: DroganFlyer GoPro mount

The UAV is controlled by a handheld wireless controller. Two joysticks control thrust, lateral movement, and yaw. Trim switches allow the user to change the sensitivity of both sticks. The center of the controller features a TFT touchscreen to connect to the UAV and configure control and video options. Important drone information is visible on this screen: roll, pitch, yaw, altitude, and battery life.

Included with our DroganFlyer system is a barebones version of DroganView software, a program that visually depicts aircraft telemetry and flight data. The unmodified main window (fig. 6) features four areas: connections (upper-right), telemetry (upper-left), flight controls (center), and data I/O (bottom). The connections area lists all computer COM ports that can support the DroganFly XBee-based transceiver. Once the correct port has been determined and selected, DroganView connects to the virtual COM port that the transceiver makes available (this is to allow direct connection to the XBee through the UART protocol). Then, a list of available drones within range is populated and can be connected. The telemetry area displays a live feed of the connected drone’s roll, pitch, yaw, attitude, altitude, throttle amount, and air speed. The flight control area allows the user to override any other controller and directly input values numerically or via sliders for the drone’s movement. The data I/O section shows the

raw and/or decrypted data stream going to the drone and coming back in.

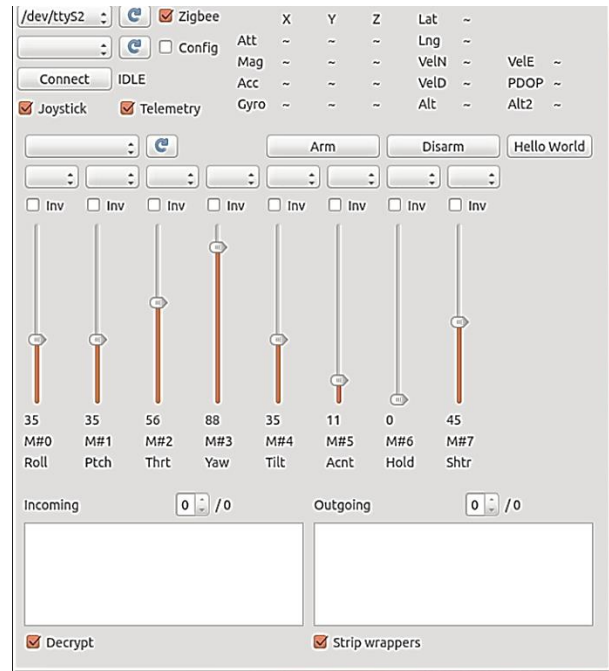


Fig. 6: Unmodified DroganView software

Source code was obtained to allow customized application programming interfaces (APIs) to be integrated into the software. DroganView is compiled from C++ using Qt 4.8.5.¹³ A new data structure was added to extract our data from DroganFly’s encrypted wireless data stream and display this data within the DroganView window in cps. This runs alongside the regular DroganView software, allowing the user to easily see incoming and outgoing drone data.

D. Transmission Methods

Without modification, the drone sends back telemetry (pitch, roll, yaw, height), and flight data (time, distance) through an encrypted wireless channel. DroganFly uses a proprietary¹⁴ message format to send data to and from the drone. The format allows for multiple types of data to be sent and includes encryption and error correction. All data to and from the drone is packaged and de/encrypted using its on-board processor. An XBee-PRO SE transmits data wirelessly at distances up to one mile through the IEEE 802.15.4

¹³ Information and documentation at <http://qt-project.org/doc/qt-4.8/>

¹⁴ This, and all information labeled “proprietary” protected under NDA

protocol.¹⁵ A USB XBee transceiver connects via USB to a computer through a VCP. The computer receives and decrypts the data using DraganView software. Data is sent and received by the transceiver. Data can be requested or sent from the transceiver in the handheld controller or connected computer.

Raw video data is sent asynchronously through a separate video transmitter. Video can be captured and streamed at up to 1080p and 60 fps. A standalone 5.8 GHz video receiver collects video data and can be ported to an analog video device or via an analog-to-USB converter.

The main board of the Guardian connects to the video camera payload to control stabilization and camera functions. An additional four pins are exposed to the end user for additional serial programming support and possible additions to sensors. Our radiation sensor was hard-wired to one of these pins to utilize the drone's 5 V logic level to interface with our counting circuit.

III. Experimental Results

Our final radiation sensor used the high-voltage kickback generator seen in fig. 6. The values specified in the Appendix were capable of producing 180-960 V.¹⁶

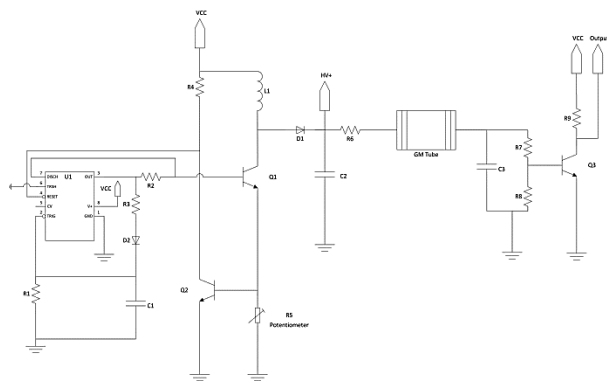


Fig. 6: Final design of kickback generator

Initial versions of this circuit used a smaller inductor (10 mH) and slower transistors (2N3904 in place of 2N4401 and FJN3303F in place of BUL7420). These were capable of producing 70-400 V, just short of the voltage needed to drive the T2417AC tube. Increasing the inductance gave a slight boost to the voltage by increasing the amount

of energy the inductor could store. This produced an increase in voltage by 75 V. After testing the circuit, it was found that the inductor was charging and discharging more slowly than desired to produce higher voltages. By changing the transistors to high-power, faster-switching devices, the on/off times were significantly decreased. By allowing Q1 to shut off faster, the inductor could discharge more quickly, effecting a larger voltage across Q1 (and then C2). By giving Q2 a faster on time, the 555 timer was able to reset more quickly, decreasing the time between pulses to turn on and off Q1. These changes were found to have the most effect on the circuit, dramatically improving the range of voltages available for use. With a maximum voltage of 960 V, this circuit could be used for any number of Geiger tubes requiring substantially lower or higher operating voltages.

Once a 575 V power supply was achieved, the full Geiger counter was tested. Before the more sensitive T2417AC tube was used, the circuit was tested with an SBM-20 tube¹⁷ produced during the Soviet era. This tube was chosen for testing due to its purported reliability and sensitivity compared to its low cost. Once it was determined that this tube functioned with the high-voltage supply and detection circuit, the T2417AC tube was tested. This tube was also capable of detecting the small amounts of beta radiation the ²⁴¹Am sample produced. Fig. 7 shows the output of the sensor for both the SBM-20 and T2417AC. The finished sensor weighed 24.0 g.

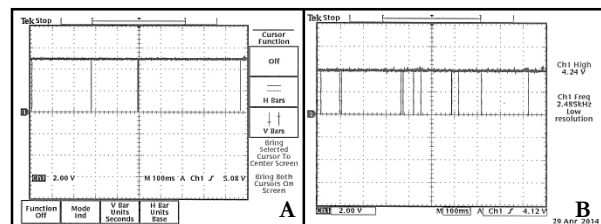


Fig. 7: Radiation sensor output for (a) SBM-20 tube and (b) T2417AC tube

The version of DraganView compiled to communicate with the drone needed to be compiled with an older version of Qt software (4.8.5 vs the newest version 5.2). To fully compile the code, we used a computer running Ubuntu 13.04. Once compiled, a custom radiation data widget was added

¹⁵ <http://standards.ieee.org/about/get/802/802.15.html>

¹⁶ See Appendix for bill of materials

¹⁷ Information at <http://www.gstube.com/data/2398/>

(fig. 8) and transceiver connectivity was successfully established.

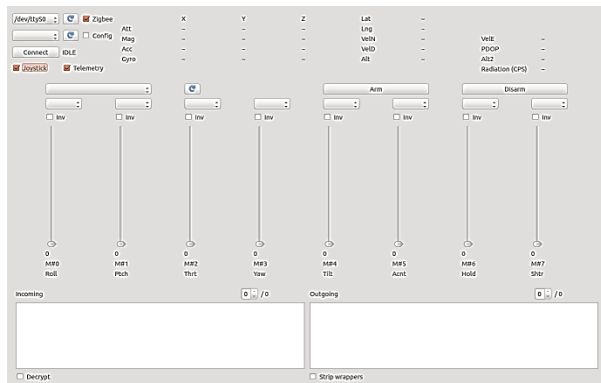


Fig. 8: Modified DraganView software window

To connect our sensor to the wired serial input of the drone, we were required to modify the drone’s firmware. To read in sensor data, the firmware was changed to use an additional read command and stream in raw binary data from a serial pin. This firmware was custom designed and programmed by DraganFly’s software engineer.

When running, the drone polled the serial pin consistently to read in sensor data by counting on falling edges (5 V to 0 V transition) and send back this count once per second. Since the sensor output was kept within 0-5 V, no additional modifications or packaging were needed before reading in the counts as bits. Computer-side, this data was read in using DraganFly’s message format and the radiation payload was identified. This payload contains a packet number to identify the time at which the signal was sent. Each packet of radiation data is checked to ensure duplicate packets are not reported. Each new non-duplicate data packet is displayed in the DraganView window beneath the drone telemetry data and updated once per second

IV. Conclusion and Future Work

Our system adds additional sensor functionality to a commercial UAV system. Drone-based systems for first response teams currently only offer optical solutions for threat detection and site surveillance. We have created a fully modular sensor package that currently supports radiation detection and can be expanded to include other digital forms of sensors. The data from our sensor is sent back wirelessly using an encrypted data channel with a range of up to one mile. With a flight time of up to 30 minutes

with our sensor mounted, the UAV system can be used to remotely investigate a potentially hazardous disaster site. By adding radiation detection, unseen radiological hazards can be detected and avoided by personnel. The capability to find radioactive areas remotely has the potential to greatly reduce the time necessary for a response team to enter and secure a disaster site, as well as protecting responders from the risks that these areas pose to human life.

Moving forward, this work can be augmented in several ways: sensor additions and miniaturization, video processing, and software improvements. The current sensor setup allows for detection and wireless transmission of radiation data in the drone’s vicinity. Now that the drone’s serial pin is exposed, multiple sensors could be used to collect more information, such as chemical or atmospheric data. By using a simple multiplexer (mux) circuit and either a hardware timer or a signal from the drone main board, many sensors could be polled by the drone using only one serial pin. The sensors could be switched on and off by the mux, alternating each second, or instead time-domain muxed to send all data simultaneously (this would require separating out the data using software after transmission). Once these new modular sensors are set up, new windows in DraganView can be created to display their data. To allow for further sensors, our radiation sensor and all future ones could be made smaller and lighter by creating custom PCBs and using surface mount components instead of the larger through-hole components used in our design. This would cut down on weight and physical space, but create issues regarding high-voltage isolation and the board’s parasitic capacitances.

Building on Davis, Pittaluga, and Panetta’s work in 2013, future revisions of our sensor package could include Human Visual System-based video processing to detect faces of known survivors in a disaster site. The drone currently only sends back an analog video signal, but many commercially available devices exist to convert this to a computer-friendly digital format via USB. Accessing the COM port of the video device and displaying it within DraganView’s window would be a simple task. Applying the algorithms present in their work can be done using the C++ MATLAB library to provide real-time video processing.

Finally, the current software version is only compatible with Linux-based computers. To improve the overall usability of our custom DraganView platform, the code can be edited to

function cross-platform and compile using Qt 5.2 (currently the latest stable version). Further revisions could include auto-detection of connected transceivers, real-time GPS (with additional GPS hardware from DraganFly) and radiation data map overlays, and the ability to import site maps for point-to-point navigation or mapping.

Acknowledgment

I would like to give special thanks to my research partner, Nicholas Davis, for all of the hard work he put into this system with me, as well as sharing his knowledge of software and communications; to Greg Wood for his instrumental role in creating our firmware and getting our drone to function; and to our research sponsor, Dr. Karen Panetta, for her immense support and continued help with this system. Thanks to Canberra Industries for helping us locate the correct Geiger tube for our project specifications.

References

- [1] N. Davis, F. Pittaluga, and K. Panetta, "Facial Recognition Using Human Visual System Algorithms for Robotic and UAV Platforms," *2013 IEEE International Conference on Technologies for Practical Robot Applications (TePRA)*, Apr 2013.
- [2] F. Ballarini, S. Altieri, S. Bortolussi, M. Carante, E. Giroletti, and N. Protti, "The BIANCA Model/Code for Radiation-Induced Cell Death: Application to Human Cells Exposed to Different Radiation Types," *Radiation and Environmental Biophysics*, Mar 2014.
- [3] E. Donnelly, J. Nemhauser, J. Smith, Z. Kazzi, E. Farfán, A. Chang, and S. Naeem, "Acute Radiation Syndrome: Assessment and Management," *Southern Medical Journal*, *103*(6), 541-546, June 2010
- [4] P. Bailey, "A First Responders Guide to Purchasing Personal Radiation Detectors (PRDs) for Homeland Security Purposes," *New York: Environmental Measurement Laboratory, U.S. Department of Homeland Security*, Nov 2004.